liquids

MDPI

Article

Development of a Test Bed to Investigate Wetting Behaviours of High-Temperature Heavy Liquid Metals for Advanced Nuclear Applications

Abhishek Saraswat [1,*,†], Rajendraprasad Bhattacharyay [1,2], Paritosh Chaudhuri [1,2] and Sateesh Gedupudi [3]

[1] Fusion Blanket Division, Institute for Plasma Research, Gandhinagar 382428, India
[2] Homi Bhabha National Institute, Training School Complex, Anushaktinagar, Mumbai 400094, India
[3] Heat Transfer and Thermal Power Laboratory, Department of Mechanical Engineering, Indian Institute of Technology Madras, Chennai 600036, India
* Correspondence: saraswat@alumni.iitm.ac.in
† Abhishek Saraswat is currently affiliated with the Department of Nuclear Science & Engineering, Massachusetts Institute of Technology, USA. The work presented in this paper was performed during his affiliation with the Fusion Blanket Division, Institute for Plasma Research, India.

Abstract

Specifically engineered heavy liquid metals are proposed as candidate coolants and tritium breeders for advanced nuclear applications. Understanding the wetting behaviours of these liquids on relevant substrate configurations is crucial to tackle the challenges associated with corrosion protection and flow diagnostics development. However, detailed investigations are scarce in the literature. In this experimental study, an apparatus is designed to measure contact angles of different liquid metals over a mirror-polished horizontal SS-304 substrate. This paper presents design aspects of the developed test facility, as well as initial results obtained using direct imaging and the Low-Bond Axisymmetric Drop Shape Analysis algorithm-based image processing technique. Methodological validation is achieved through surrogate liquids/liquid metals (H_2O, Hg, Ga, GaInSn), prior to taking measurements from molten lead (Pb) droplets at 425 °C. Estimated contact angles obtained using the two techniques lie within ±10% deviation. Towards the end, the paper lays out plans for future upgrades for studies of wetting behaviours of molten Pb/Pb alloys on substrates with relevant surface properties, including bare P-91 and reduced-activation ferritic–martensitic steels, along with Al_2O_3/Er_2O_3-coated versions of these materials, to generate a database for Gen-IV fission reactors and fusion power plants.

Keywords: liquid metal; contact angle; wettability; sessile drop; interface

check for updates

Academic Editor: Zareen Abbas

Received: 27 October 2025
Revised: 17 November 2025
Accepted: 24 November 2025
Published: 26 November 2025

Citation: Saraswat, A.; Bhattacharyay, R.; Chaudhuri, P.; Gedupudi, S. Development of a Test Bed to Investigate Wetting Behaviours of High-Temperature Heavy Liquid Metals for Advanced Nuclear Applications. *Liquids* **2025**, *5*, 33. https://doi.org/10.3390/liquids5040033

Copyright: © 2025 by the authors. Licensee MDPI, Basel, Switzerland. This article is an open access article distributed under the terms and conditions of the Creative Commons Attribution (CC BY) license (https://creativecommons.org/licenses/by/4.0/).

1. Introduction

Heavy liquid metals (HLMs) such as molten lead (Pb) and its alloys (PbLi, PbBi, etc.) are preferred candidates for coolants, neutron multipliers, and tritium breeders in advanced fission and fusion reactor concepts due to several technological advantages such as high boiling point (>1400 °C), low vapor pressure, excellent thermal conductivity, and reduced chemical activity towards H_2O and air, as well as the economic advantage of abundance [1–3].

However, molten Pb—an active corrodant—selectively leaches out elemental constituents (like Ni and Cr) over extended operational durations, leading to compromised structural integrity in vital components [4]. The corrosion behaviour of an LM is influenced by its wetting nature towards a substrate, leading to a higher degree of LM embrittlement

with higher wettability [5]. One of the routes proposed to enhance the longevity of such components is implementation of a surface barrier in the form of functional oxides (ceramic coatings), physically decoupling the LM from the steel matrix [6,7]. At the other end of this spectrum, efficient operations for these HLM circuits and associated safety interlocks are facilitated by accurate flow measurements, which are constrained by process conditions such as a high temperature, a corrosive nature, and an opacity of LM flows [8]. Ultrasonic flow velocimetry and electromagnetic flow measurements emerge as attractive choices, with their performance being primarily governed by efficient acoustic coupling and minimal contact resistance, respectively, between the flow pipe and the HLM of interest [1,9]. Associated challenges as well as progress made on this front have been reported in several studies for Pb-based melts [10–12].

The abovementioned discussions establish the perspective that, in nuclear applications, corrosion protection and the deployment of diagnostics are highly impacted by the wetting characteristics of the LM–substrate pair under consideration. These two requirements, however, may not necessarily be synergistic, as the structural materials exhibiting LM compatibility (relevant to flow sections outside the reactor) are seldom suitable for utilization in the high-radiation, high-temperature environment inside the reactor due to concerns such as long-term radiation activation. In view of the significant efforts being made worldwide towards qualification of structural and functional materials [13,14], there is now a pressing requirement for a relevant experimental database for the effective screening of candidate materials which will enable a faster route to further exhaustive investigations.

To advance current understanding of the wetting behaviours of Pb-based melts, a contact angle (θ) measurement test facility was developed at the Institute for Plasma Research (IPR), India. Liquid–solid interfaces and the overall shapes of sessile (static) LM droplets placed on a horizontal SS-304 substrate were analysed through direct imaging and the Low-Bond Axisymmetric Drop Shape Analysis (LBADSA) image processing technique, to study wettability. To the best knowledge of the authors, the LBADSA tool has not been utilized in previous studies to investigate the wetting characteristics of HLMs such as Pb/Pb-alloys—a class of coolants and breeders of interest in the domain of advanced nuclear engineering.

2. Materials and Methods

The wettability of a solid–liquid pair is defined by the contact angle (θ)—the angle between the solid–liquid interface and the liquid–vapor interface, as shown in Figure 1. The equilibrium condition for a sessile drop is defined by the Young's equation correlating the forces of cohesion and adhesion, expressed as follows:

$$\gamma_{SV} = \gamma_{SL} + \gamma_{LV}\, cos\theta \quad (1)$$

where the subscripts S, L, and V define the solid, liquid, and vapor phases, respectively, while γ defines the interfacial free energy between these phases. The magnitude of θ indicates the preference of a liquid to spread over a given solid surface.

The present study exploits experimental estimations of contact angles to establish the wettability of different liquid–SS pairs. To achieve this aim, a metallographically mirror-polished SS-304 substrate of 50 mm width is prepared using FEPA grit #80 to #4000 SiC papers on Struers LaboPol-25 (Copenhagen, Denmark). The polished substrate is ultrasonically cleaned with acetone for a duration of 10 min, followed by a 30 min drying period. The polishing and cleaning steps mentioned above are repeated after each experiment to maintain a clean surface. Horizontal placement of the prepared substrate is ensured using a spirit level. For H_2O and room-temperature LMs (Hg, Ga, GaInSn), dedicated 24-gauge Stainless Steel (SS) hypodermic needles (ID ~0.31 mm) are used to

position drop(s) near the edge of the substrate, at an ambient temperature of 27–35 °C, as shown in Figure 2a. Selection of needle material is primarily governed by the excellent chemical compatibility of SS with Hg and Ga/GaInSn at room temperature [15,16]. To avoid any cross-contamination, separate needles are used for dispensing different LMs. Direct imaging of the liquid–solid interface (Figure 2b) is performed through a 24X macro lens with 10 mm shooting distance. For each drop, 5 or 6 separate images are captured to arrive at a mean value of the contact angle. To generate molten Pb drops, 99.98% purity Pb shots of 2 mm diameter are cleaned for surface oxidation, followed by melting in an inert (Ar) environment. The utilized test set-up with heating arrangement for molten Pb is depicted in Figure 3.

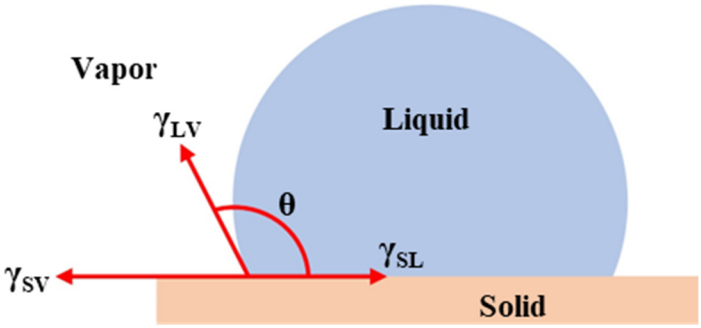


Figure 1. Equilibrium condition for a sessile drop, and definition of a contact angle.

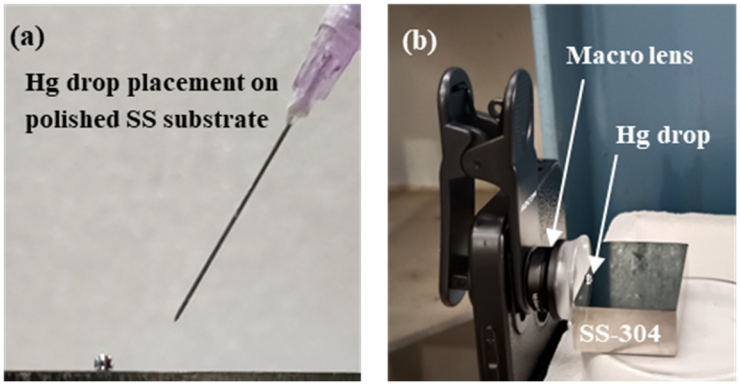


Figure 2. (**a**) Placement of a mercury (Hg) drop at the edge of substrate; (**b**) image capturing for Hg drop.

The test set-up consists of a 0.45 kW ceramic band heater covering a solid Cu heat flux smoother (r = 25 mm; l = 60 mm), over which the SS substrate is placed. During operation, heat conducted through the smoother melts the Pb shot(s) located on the substrate surface. An SS-316 sheathed K-type thermocouple, calibrated according to IEC 60584 (https://webstore.iec.ch/en/publication/2521 accessed on 27 October 2025) Class I accuracy, is used to provide feedback control for the heater. Another thermocouple spot-welded to the substrate surface provides continuous monitoring of the temperature to which the melt drops are exposed. The complete assembly is enclosed by a clear glass vessel placed over multiple layers of thermal insulation consisting of fused silica sheets and a cerawool blanket. Continuous Ar purging helps maintain an inert environment over the LM to avoid oxidation, while the swaying fibres attached to the Ar injection nozzle (refer to Figure 3) provide visual indication of a maintained Ar flow.

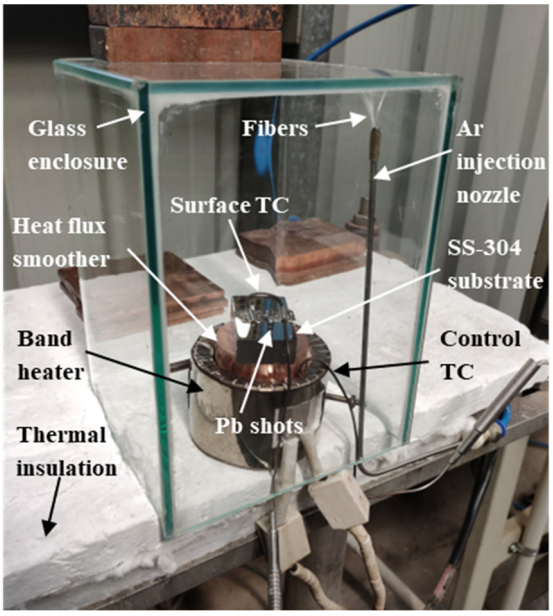


Figure 3. Contact angle measurement test set-up for high-temperature melts (present case: molten Pb).

Two methods are utilized to estimate the contact angle θ: (i) direct imaging coupled with an online protractor tool; and (ii) LBADSA algorithm-based image processing—a model derived from a first-order perturbation solution to the Young–Laplace equation for axisymmetric sessile drops [17]. The LBADSA approach allows measurement of contact angles and surface tensions within enveloping assumptions of a low Bond number (*Bo*) to simplify mathematical modelling for a spherical drop shape. In this approach, a small perturbation solution based on the Young–Laplace equation is fitted to the drop contour and optimized using image energy gradients—providing a significant advantage in drop edge detection for applications with noisy images. Detailed information on this technique is available under [17]. The captured images are converted to an 8-bit format, and subsequently processed in the ImageJ software (ImageJ version 1.47) for analysis via the LBADSA tool. Direct-imaging-based estimations report the contact angle at the left end of an analysed drop under the assumption of a symmetric drop, while the LBADSA tool provides an average of contact angles measured at both ends of the analysed drop. The primary motivation for exploration of the LBADSA technique is its effectiveness in aiding study of high-temperature heavy LMs of interest to advance nuclear applications. Potentially, it may provide a cost-effective tool for study of LMs and molten salts of relevance to nuclear engineering applications, for which commercial off-the-shelf solutions are few.

3. Results and Discussion

This section presents results and inferences derived from the experimental investigations on H_2O/LM–substrate pairs.

3.1. Room-Temperature Measurements

Initial measurements are performed using De-Ionized (DI) water drops placed on the prepared SS-304 substrate. Captured images of the liquid–solid interface and its LBADSA-processed version are depicted in Figures 4a and 4b, respectively. These results are in good agreement with the reported values for H_2O/SS systems, varying from 60° to 65°, suggesting a modest wettability for this pair [18–20]. Estimated values of $\theta_{H2O/SS}$ averaged over five measurements obtained using the two techniques are 59.00° ± 1.22° and 61.09° ± 2.05°, respectively, providing a deviation of ~3.5%.

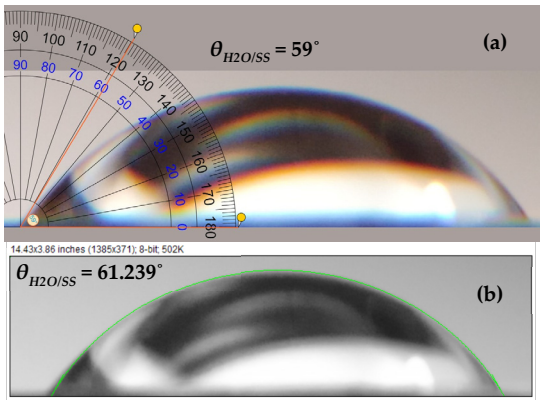


Figure 4. Contact angle estimation for the DI-H_2O/SS-304 pair using (**a**) the direct imaging method; and (**b**) image processing based on the LBADSA algorithm.

With encouraging results from the DI-H_2O case, the applicability of the method is extended to low-melting LMs, including commercial-grade Hg (>99.9%), high-purity Ga (>99.999%) and commercial GaInSn (unknown purity), captured and corresponding processed 8-bit images for which are presented in Figure 5a,b, Figure 6a,b, and Figure 7a,b, respectively. Average contact angles estimated from the room-temperature investigations are summarized in Table 1.

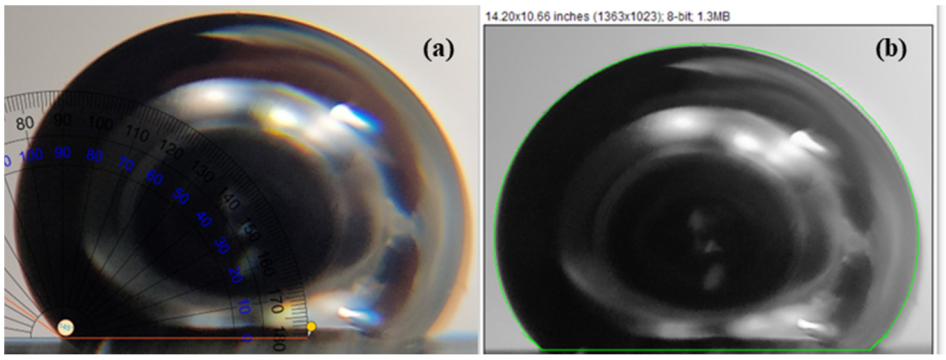


Figure 5. Contact angle estimation for the Hg/SS-304 pair using (**a**) the direct imaging method; and (**b**) image processing based on the LBADSA algorithm.

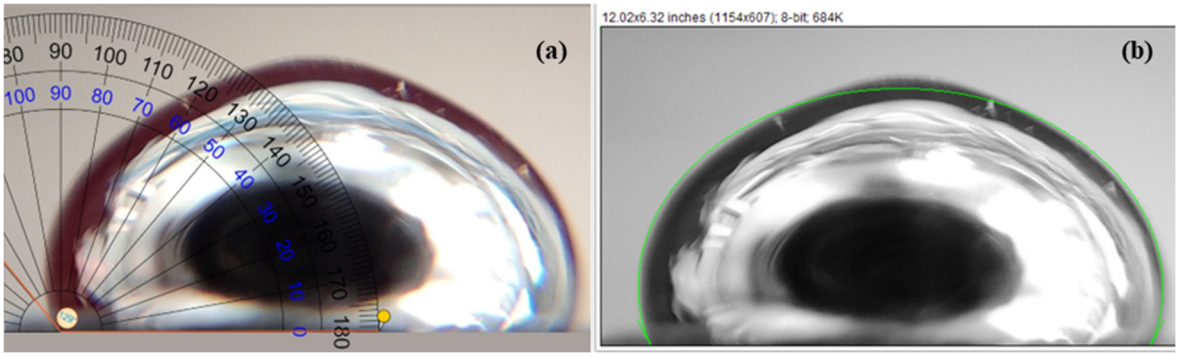


Figure 6. Contact angle estimation for the Ga/SS-304 pair using (**a**) the direct imaging method; and (**b**) image processing based on the LBADSA algorithm.

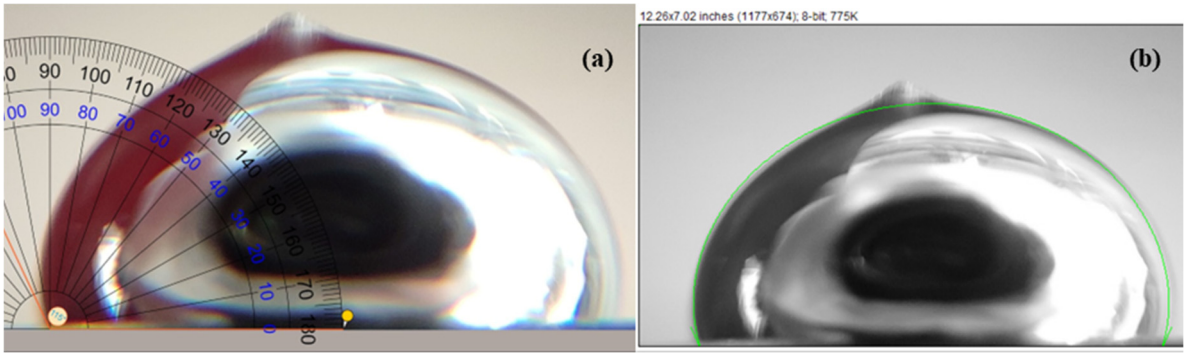


Figure 7. Contact angle estimation for the GaInSn/SS-304 pair using (**a**) the direct imaging method; and (**b**) image processing based on the LBADSA algorithm.

Table 1. Summary of contact angle measurements.

Pair	$\theta_{Direct\ imaging}$	θ_{LBADSA}	% Deviation
H_2O/SS	59.00° ± 1.22°	61.09° ± 2.05°	3.54
Hg/SS	149.67° ± 3.27°	136.10° ± 4.41°	−9.07
Ga/SS	129.33° ± 3.39°	119.72° ± 0.80°	−7.43
GaInSn/SS	115.83° ± 1.83°	114.79° ± 1.40°	−0.90

Results for the Hg/SS pair, suggesting poor wettability, conform with ranges reported in the existing literature [21,22]. However, the relatively larger deviation between the estimated contact angles for the Hg/SS pair obtained using the two techniques may arise from an inherent assumption of a low *Bo* in LBADSA. This observation highlights the practical uncertainties expected from when the tool is employed for HLMs. Considering an acceptable error limit of ±7% for the algorithm on synthetic drops, as reported in [17], the results obtained in the present study are encouraging for high-density liquids. One particularly striking observation is the difficulty of dispensing Ga/GaInSn drops, compared to Hg. Multiple attempts repeatedly resulted in a distorted (pointed) shape for these drops even at an ambient temperature (~32 °C) higher than the melting points of both Ga and GaInSn. This effect is completely absent in Hg, and is less pronounced for the utilized Ga drop, as compared to that for GaInSn. This could also be observed from drop portions protruding out of the green contours for the three LMs (refer to Figures 5–7). It should also be noted that initial drops for Ga exhibited behaviour highly similar to that of GaInSn. Owing to their high surface tension (>400 mN/m), LMs tend to form spherical drops, minimizing the surface area. However, presence of an enveloping oxide layer can impart rigidity and viscoelasticity to the drop, enabling a stable non-spherical shape. Hg metal is relatively sluggish towards oxidation in air at room temperature under the time duration of interest for this study, while temperature in excess of 250 °C can accelerate oxidation [23]. In contrast, Ga/Ga-based alloys react rapidly to form a nanometre-thin Ga_2O_3 surface layer even at ambient conditions. This observation is consistent with previous studies [24,25] suggesting oxidation as the principal cause of such distortion, which results in Ga/Ga-based alloys exhibiting gel-like behaviour. As reported in [26], any oxygen concentration above 1 ppm will result in rapid surface oxidation owing to the high affinity of Ga towards O_2.

As all the room-temperature experiments in this study are conducted in an open atmosphere, these deformations are unavoidable. A set of two successive drops dispensed from the needle is shown in Figure 8. In consideration of its lesser degree of distortion, Drop-2 is selected for contact angle analysis in this study (refer to Figure 7). For both Ga and GaInSn, suction-enabled removal of drop(s) using a hypodermic needle resulted in

a residual sticky layer, as shown in Figure 9. This is likely due to an interaction between the LM oxide film and the SS surface. This observation, in close agreement with [24], affirms the presence of an adhesive Ga_2O_3 oxide layer encapsulating the drop surface, thus suppressing the retraction and rebound characteristics to stabilize a non-spherical drop shape.

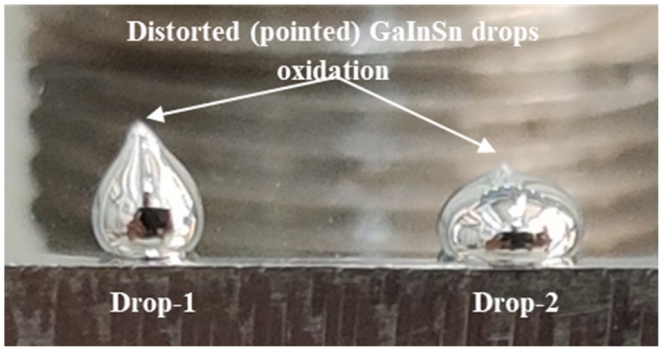


Figure 8. Distorted shapes of GaInSn alloy drops owing to rapid surface oxidation.

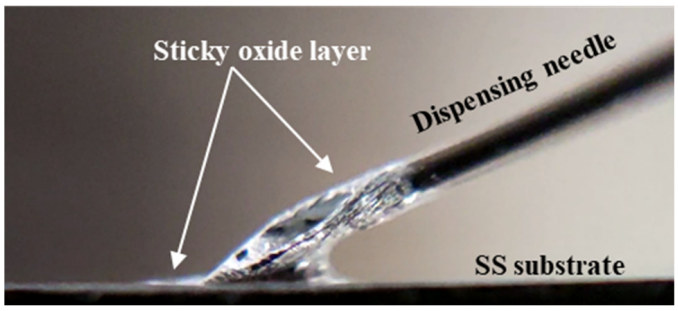


Figure 9. Oxide layer on the substrate and the dispensing needle tip during GaInSn drop collection.

Considering the satisfactory validation of direct imaging and LBADSA techniques on water–SS and Hg–SS pairs, it could be inferred that the contact angle made by GaInSn Drop-2 in this study is still correctly captured, considering the much lower deviation (<1%) in the results produced by the two techniques. However, this may not reliably translate to actual wetting behaviours of static Ga/GaInSn drops with no oxidation. Further detailed investigations with stringent chemistry control are necessary. The obtained results for Ga/GaInSn must be used with caution, owing to the non-deterministic behaviour of the surface oxide layer which could allow drop shape manipulation in different non-equilibrium but stable morphologies [27,28].

3.2. High-Temperature Measurements for Molten Pb

The assembled facility (shown in Figure 3) was utilized to study SS wetting by Pb drops generated by melting solid Pb shots. Figure 10 presents raw and processed images of Pb drops used to analyse $\theta_{Pb/SS}$. One of the major challenges encountered during high-temperature investigations was the required distance between the image capturing equipment and the Pb drop, because of which the macro lens could not be deployed. This may result in some blurring at the droplet surface boundary, contributing to inaccuracies in estimated contact angles.

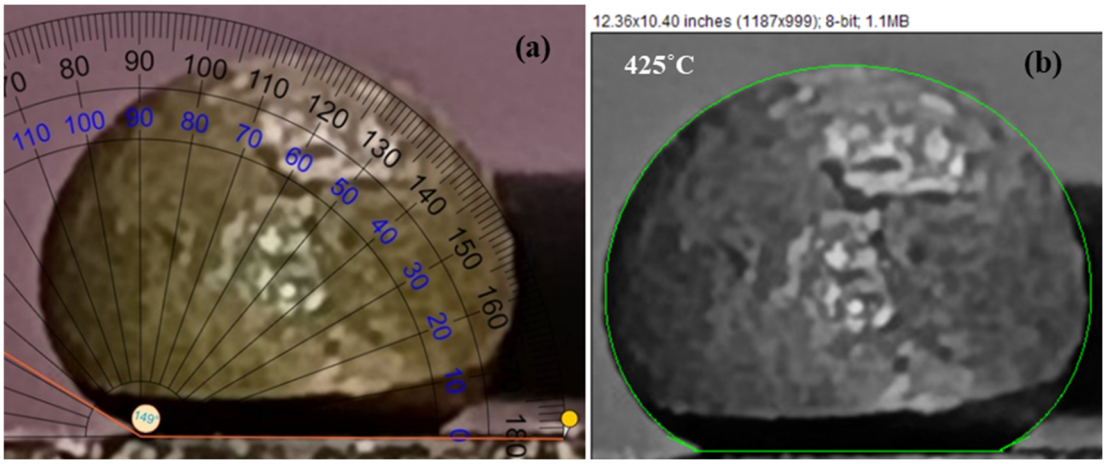


Figure 10. Contact angle estimation for the molten Pb/SS-304 pair at 425 °C using (**a**) the direct imaging method; and (**b**) image processing based on the LBADSA algorithm.

Further, although Pb shots were manually cleaned to remove the surface oxide layer prior to melting under an inert atmosphere of flowing Ar, an oxide layer gradually appeared—as evidenced by the absence of a smooth drop surface (refer to Figure 10). This could have resulted from a trace amount of O_2 present in the utilized Ar supply, outgassing from components at higher temperature, or an ineffective/partial displacement of pre-existing air through Ar purging of glass chamber. Estimated average values of $\theta_{Pb/SS}$ for the surface-oxidized molten Pb drops (at 425 °C) over six separate measurements were 151.17° ± 1.60° and 156.14° ± 2.20° using direct imaging and LBADSA, respectively, suggesting a deviation of ~3.29% between the two techniques. The observed poor wettability of SS-304 by molten Pb is in good agreement with reported contact angle values varying between 143° and 150° over an operating temperature of 350–600 °C for surface-oxidized Pb drops [29,30]. This poor wettability could be attributed to a coupled effect of a PbO layer forming on the drop and a passivating oxide layer forming on the SS substrate at higher temperatures.

In addition, it was noticed that a slight manual tapping could aid in detachment of the oxide layer, at least partially, without altering the shape of the Pb drops. However, in the present study, such a manoeuvre repeatedly led to surface oxidation owing to atmospheric exposure at higher temperature. Molten Pb without surface oxides is expected to exhibit better wettability (θ ~ 90°) with SS substrates [31]; this is representative of reactor-relevant scenarios considering the use of separate melt tanks to remove floating oxides, melting and charging in an inert (Ar/He) atmosphere, and active removal of oxide impurities from flow circuits. Replication of similar conditions in the set-up would necessitate upgrades, as discussed in in Section 4, to allow for stringent controls on oxygen specifications (<0.31 wt.-ppm) [32]. However, the good agreement with the available data for surface-oxidized molten Pb drops confirms the applicability of the adopted methodology for practical estimations.

3.3. Sources of Uncertainties

Exploration of LBADSA-algorithm-assisted wettability quantification is primarily motivated by its ease of use, rigorously validated performance, and open-source availability. Both the utilized techniques suggest the same trend for wettability, as follows:

$$\theta_{H2O/SS} < \theta_{GaInSn/SS} < \theta_{Ga/SS} < \theta_{Hg/SS} < \theta_{Pb/SS}$$

Table 1 clearly depicts an underestimation of contact angles for low-melting LMs by the LBADSA algorithm. Moreover, the direct imaging technique tends to produce results in agreement with those of previous studies, as discussed in Sections 3.1 and 3.2. It is worth highlighting that, for a given liquid–SS pair, the same images are used to estimate the average contact angle in both the techniques, thus eliminating possible effects of variations in environmental factors and substrate surface properties. The observed deviation could partly be attributed to reliance on a first-order perturbation solution in the LBADSA approach approximating the drop profile to a circular one [17]. Moreover, generating the drop contour based on image energy in LBADSA may lead to an inherent inaccuracy when coupled with technical limitations (resolution, contrast, optical distortion, etc.) of the image capturing components. In light of this, no image correction/enhancements are performed in the present study except for an 8-bit conversion necessitated by the LBADSA plug-in module. It should also be mentioned that drop size is not expected to be a significant factor contributing to error, as the LBADSA algorithm is rigorously validated for drop diameters up to 6 mm and contact angles up to 180°, enveloping the complete range of wetting media utilized in the present study [17]. However, drop fluid density may introduce some degree of error, as gravity and surface tension are the only competing forces governing the shape of a sessile drop. The Bond number (*Bo*), depicting the relative strength of gravitational force to the surface tension effects, is defined as

$$Bo = \frac{\Delta\rho g {R_0}^2}{\sigma} \tag{2}$$

where $\Delta\rho$, g, R_0, and σ are the density difference between displacing and displaced fluids, gravitational acceleration, characteristic length and surface tension, respectively. A high *Bo* indicates a prominent effect of gravity, leading to distortion from a spherical drop shape. Therefore, for a high-density liquid, shape distortion (flattening) under the influence of gravity could partially invalidate the assumption of a low Bond number. The liquids utilized in this work are LMs of much higher density compared to ordinary fluids and the fluids used in the previous study [17]. As the present study employs a mirror-polished substrate for each investigation, the automatic and accurate baseline detection feature of LBADSA (using drop reflection) helps minimize the uncertainties creeping from an inaccurate interface detection. Still, factors such as a relative tilt between the substrate and the camera and a lack of axial symmetry in the produced drops could potentially affect the accuracy of results derived using a complete drop shape in LBADSA. In contrast, estimations at the three-phase boundary point in direct imaging methodology lower the uncertainty resulting from a lack of drop symmetry. A few studies have highlighted sample-dependent variations from the LBADSA algorithm [33].

4. Conclusions

A test facility was designed at IPR to assess the wettability characteristics of various liquid metals of interest in the domain of nuclear engineering. Methodological validation was successfully achieved by using LMs with well-studied wetting behaviours, including molten Pb at 425 °C. Preliminary results suggest an under-estimation of contact angles using LBADSA, an observation possibly resulting from the limited applicability of assuming a low Bond number for HLMs. Further investigations are needed to confirm these observations. Inferences derived from the analyses of sessile Ga/GaInSn drops suggest a non-equilibrium morphology and the possibility of shape manipulation in the presence of surface oxide layers. As suggested in earlier studies [34], the reliability of estimated contact angles for Ga/Ga-based alloys remains questionable in the absence of stringent oxygen control. This facility is expected to be utilized to study LM–substrate pairs for which wettability data

is either scarce or inexistent. A few such pairs worth mentioning include Pb/PbLi-P91, Pb/PbLi–Reduced-Activation Ferritic-Martensitic Steel (RAFMS), Pb/PbLi-Al_2O_3-coated SS/RAFMS, Pb/PbLi-Er_2O_3-coated SS/RAFMS, etc. Upgrade plans for the facility include incorporating a glove box to enable tighter surface-chemistry control, thereby avoiding oxidation during material handling and during investigations at high temperatures. A high-resolution image capturing system is foreseen to study the temporal evolution of wetting behaviour in a thermal steady state as well as temperature-governed wetting behaviour over operational durations to address the screening of structural/functional materials for LM corrosion compatibility. An improved dispenser to repeatedly produce LM drops of controlled volume is indispensable for the reproducibility of experiments. Necessary efforts are in progress on this front elsewhere [35,36]. At an advanced stage, the facility will be equipped with a servo-controlled tilting arrangement to allow investigations for advancing and receding angles. This data would be utilized with the aim of selecting materials for the development of contact-type two-phase detection diagnostics in consideration of the sensor response dictated by LM wetting/de-wetting characteristics.

Author Contributions: Conceptualization, A.S.; Methodology, A.S. and S.G.; Investigation, A.S.; Formal analysis, A.S.; Resources, R.B. and P.C.; Data curation, A.S.; Writing—original draft, A.S.; Writing—review and editing, R.B. and S.G.; Supervision, R.B. and P.C. All authors have read and agreed to the published version of the manuscript.

Funding: This research received no external funding.

Data Availability Statement: The original contributions presented in this study are included in the article. Further inquiries can be directed to the corresponding author.

Acknowledgments: The authors would like to thank Hardik Taylor (IPR) for his technical guidance on metallographic preparations. The authors also appreciate the inputs provided by Maulik Panchal (IPR) relating to the heating arrangements of the assembly.

Conflicts of Interest: The authors declare no conflicts of interest.

References

1. Nuclear Energy Agency. *Handbook on Lead-Bismuth Eutectic Alloy and Lead Properties, Materials Compatibility, Thermal-Hydraulics and Technologies*; No. 7268; NEA: Paris, France, 2015.
2. Weeks, J.R. Lead, Bismuth, Tin and Their Alloys as Nuclear Coolants. *Nucl. Eng. Des.* **1971**, *15*, 363–372. [CrossRef]
3. Arena, P.; Del Nevo, A.; Moro, F.; Noce, S.; Mozzillo, R.; Imbriani, V.; Giannetti, F.; Edemetti, F.; Froio, A.; Savoldi, L.; et al. The DEMO Water-Cooled Lead–Lithium Breeding Blanket: Design Status at the End of the Pre-Conceptual Design Phase. *Appl. Sci.* **2021**, *11*, 11592. [CrossRef]
4. Zhang, J. A Review of Steel Corrosion by Liquid Lead and Lead–Bismuth. *Corros. Sci.* **2009**, *51*, 1207–1227. [CrossRef]
5. Wang, W.; Yang, C.; You, Y.; Yin, H. A Review of Corrosion Behavior of Structural Steel in Liquid Lead–Bismuth Eutectic. *Crystals* **2023**, *13*, 968. [CrossRef]
6. Saraswat, A.; Sasmal, C.; Prajapati, A.; Bhattacharyay, R.; Chaudhuri, P.; Gedupudi, S. Experimental Investigations on Electrical-Insulation Performance of Al_2O_3 Coatings for High Temperature PbLi Liquid Metal Applications. *Ann. Nucl. Energy* **2022**, *167*, 108856. [CrossRef]
7. Priya, R.; Ningshen, S. Corrosion Behaviour of P-91 Steel and Type 316 LN Stainless Steel with and Without a Ceramic Coating in the Lead with Oxygen at 550 °C. *J. Nucl. Mater.* **2023**, *574*, 154181. [CrossRef]
8. Saraswat, A.; Fraile, A.; Gedupudi, S.; Bhattacharyay, R.; Chaudhuri, P. A Comprehensive Review of Experimental and Numerical Studies on Liquid Metal-Gas Two-Phase Flows and Associated Measurement Challenges. *Ann. Nucl. Energy* **2025**, *213*, 111104. [CrossRef]
9. Hawes, J.; Knapp, J.; Burrows, R.; Montague, R.; Arndt, J.; Walters, S. Achieving Wetting in Molten Lead for Ultrasonic Applications. *Nucl. Eng. Technol.* **2024**, *56*, 437–443. [CrossRef]
10. Smolentsev, S.; Li, F.-C.; Morley, N.; Ueki, Y.; Abdou, M.; Sketchley, T. Construction and Initial Operation of MHD PbLi Facility at UCLA. *Fusion Eng. Des.* **2013**, *88*, 317–326. [CrossRef]

11. Ueki, Y.; Hirabayashi, M.; Kunugi, T.; Nagai, K.; Saito, J.; Ara, K.; Morley, N.B. Velocity Profile Measurement of Lead-Lithium Flows by High-Temperature Ultrasonic Doppler Velocimetry. *Fusion Sci. Technol.* **2011**, *60*, 506–510. [CrossRef]
12. Wetzel, T. Instrumentation. In *Handbook on Lead-Bismuth Eutectic Alloy and Lead Properties, Materials Compatibility, Thermal-Hydraulics and Technologies*; No. 7268; Nuclear Energy Agency NEA: Paris, France, 2015; Chapter 11, pp. 731–839.
13. Zinkle, S.J.; Busby, J.T. Structural Materials for Fission & Fusion Energy. *Mater. Today* **2009**, *12*, 12–19. [CrossRef]
14. Odette, G.R.; Zinkle, S.J. *Structural Alloys for Nuclear Energy Applications*; Elsevier: Amsterdam, The Netherlands, 2019.
15. Narh, K.A.; Dwivedi, V.P.; Grow, J.M.; Stana, A.; Shih, W.-Y. The Effect of Liquid Gallium on the Strengths of Stainless Steel and Thermoplastics. *J. Mater. Sci.* **1998**, *33*, 329–337. [CrossRef]
16. Pawel, S.J. *Summary of Mercury Compatibility Issues for the Spallation Neutron Source Target Containment and Ancillary Equipment*; ORNL/TM-2002/280; Oak Ridge National Laboratory: Oak Ridge, TN, USA, 2002.
17. Stalder, A.F.; Melchior, T.; Müller, M.; Sage, D.; Blu, T.; Unser, M. Low-Bond Axisymmetric Drop Shape Analysis for Surface Tension and Contact Angle Measurements of Sessile Drops. *Colloids Surf. A Physicochem. Eng. Asp.* **2010**, *364*, 72–81. [CrossRef]
18. Martinez-Urrutia, A.; de Arroiabe, P.F.; Ramirez, M.; Martinez-Agirre, M.; Bou-Ali, M.M. Contact Angle Measurement for LiBr Aqueous Solutions on Different Surface Materials Used in Absorption Systems. *Int. J. Refrig.* **2018**, *95*, 182–188. [CrossRef]
19. Kubiak, K.J.; Wilson, M.C.T.; Mathia, T.G.; Carval, P. Wettability Versus Roughness of Engineering Surfaces. *Wear* **2011**, *271*, 523–528. [CrossRef]
20. Somlyai-Sipos, L.; Baumli, P. Wettability of Metals by Water. *Metals* **2022**, *12*, 1274. [CrossRef]
21. Wilkinson, M.C. Surface Properties of Mercury. *Chem. Rev.* **1972**, *72*, 575–625. [CrossRef]
22. Ellison, A.H.; Klemm, R.B.; Schwartz, A.M.; Grubb, L.S.; Petrash, D.A. Contact Angles of Mercury on Various Surfaces and the Effect of Temperature. *J. Chem. Eng. Data* **1967**, *12*, 607–609. [CrossRef]
23. Rallo, M.; Heidel, B.; Brechtel, K.; Maroto-Valer, M.M. Effect of SCR Operation Variables on Mercury Speciation. *Chem. Eng. J.* **2012**, *198–199*, 87–94. [CrossRef]
24. Du, J.; Wang, X.; Li, Y.; Min, Q. How an Oxide Layer Influences the Impact Dynamics of Galinstan Droplets on a Superhydrophobic Surface. *Langmuir* **2022**, *38*, 5645–5655. [CrossRef] [PubMed]
25. Davis, E.A. On the Wetting States of Low Melting Point Metal Galinstan and Wetting Characteristics of 3-Dimensional Nanostructured Fractal Surfaces. Master's Thesis, Mechanical and Materials Engineering Department, University of Nebraska, Lincoln, NE, USA, 2017.
26. Liu, T.; Sen, P.; Kim, C.-J. Characterization of Nontoxic Liquid-Metal Alloy Galinstan for Applications in Microdevices. *J. Microelectromech. Syst.* **2012**, *21*, 443–450. [CrossRef]
27. Joshipura, I.D.; Persson, K.A.; Truong, V.K.; Oh, J.-H.; Kong, M.; Vong, M.H.; Ni, C.; Alsafatwi, M.; Parekh, D.P.; Zhao, H.; et al. Are Contact Angle Measurements Useful for Oxide-Coated Liquid Metals? *Langmuir* **2021**, *37*, 10914–10923. [CrossRef]
28. Dickey, M.D. Emerging Applications of Liquid Metals Featuring Surface Oxides. *ACS Appl. Mater. Interfaces* **2014**, *6*, 18369–18379. [CrossRef] [PubMed]
29. Eustathopoulos, N.; Sobczak, N.; Passerone, A.; Nogi, K. Measurement of Contact Angle and Work of Adhesion at High Temperature. *J. Mater. Sci.* **2005**, *40*, 2271–2280. [CrossRef]
30. Giuranno, D.; Gnecco, F.; Ricci, E.; Novakovic, R. Surface Tension and Wetting Behaviour of Molten Bi–Pb Alloys. *Intermetallics* **2003**, *11*, 1313–1317. [CrossRef]
31. Protsenko, P.; Terlain, A.; Jeymond, M.; Eustathopoulos, N. Wetting of Fe–7.5%Cr Steel by Molten Pb and Pb–17Li. *J. Nucl. Mater.* **2002**, *307–311 Pt 2*, 1396–1399. [CrossRef]
32. Courouau, J.L. Chemistry Control and Monitoring Systems. In *Handbook on Lead-Bismuth Eutectic Alloy and Lead Properties, Materials Compatibility, Thermal-Hydraulics and Technologies*; No. 7268; Nuclear Energy Agency NEA: Paris, France, 2015; Chapter 4, pp. 185–238.
33. Williams, D.L.; Kuhn, A.T.; Amann, M.A.; Hausinger, M.B.; Konarik, M.M.; Nesselrode, E.I. Computerised Measurement of Contact Angles. *Galvanotechnik* **2010**, *101*, 2502–2512.
34. Handschuh-Wang, S.; Gan, T.; Wang, T.; Stadler, F.J.; Zhou, X. Surface Tension of the Oxide Skin of Gallium-Based Liquid Metals. *Langmuir* **2021**, *37*, 9017–9025. [CrossRef]
35. Shone, A.; Koyn, Z.; Kamiyama, B.; Perez, E.; Barrus, L.; Bartlett, N.; Allain, J.P.; Andruczyk, D. HIDRA-MAT Liquid Metal Droplet Injector for Liquid Metal Applications in HIDRA. *Fusion Eng. Des.* **2022**, *180*, 113193. [CrossRef]
36. Pérez, C.L.; Marchhart, T.; Kawashimo, K.; Nieto-Perez, M.; Parsons, M.S.; Schamis, H.; Allain, J.P. A Liquid Metal Dropper for Experiments on the Wettability of Liquid Metals on Plasma Facing Components. *Rev. Sci. Instrum.* **2023**, *94*, 103506. [CrossRef]

Disclaimer/Publisher's Note: The statements, opinions and data contained in all publications are solely those of the individual author(s) and contributor(s) and not of MDPI and/or the editor(s). MDPI and/or the editor(s) disclaim responsibility for any injury to people or property resulting from any ideas, methods, instructions or products referred to in the content.